

## Improved solubility, dissolution rate, and oral bioavailability of main biflavonoids from *Selaginella doederleinii* extract by amorphous solid dispersion

Bing Chen<sup>a,b,c,\*</sup>, Xuewen Wang<sup>b,c,\*</sup>, Yanyan Zhang<sup>b,c</sup>, Kangping Huang<sup>b,c</sup>, Hao Liu<sup>b,c</sup>, Dafen Xu<sup>b,c</sup>, Shaoguang Li<sup>b,c</sup>, Qicai Liu<sup>a,b</sup>, Jianyong Huang<sup>d</sup>, Hong Yao<sup>b,c,e</sup> and Xinhua Lin<sup>a,b,c</sup>

<sup>a</sup>Nano Medical Technology Research Institute, Fujian Medical University, Fuzhou, China; <sup>b</sup>Higher Educational Key Laboratory for Nano Biomedical Technology of Fujian Province, Fujian Medical University, Fuzhou, China; <sup>c</sup>Department of Pharmaceutical Analysis, School of Pharmacy, Fujian Medical University, Fuzhou, China; <sup>d</sup>Department of Pharmaceutical, Fujian Medical University Union Hospital, Fuzhou, China; <sup>e</sup>Fujian Key Laboratory of Drug Target Discovery and Structural and Functional Research, Fujian Medical University, Fuzhou, China

### ABSTRACT

Amentoflavone, robustaflavone, 2'',3''-dihydro-3',3'''-biapigenin, 3',3'''-binaringenin, and delicaflavone are five major hydrophobic components in the total biflavonoids extract from *Selaginella doederleinii* (TBESD) that display favorable anticancer properties. The purpose of this study was to develop a new oral delivery formulation to improve the solubilities, dissolution rates, and oral bioavailabilities of the main ingredients in TBESD by the solid dispersion technique. Solid dispersions of TBESD with various hydrophilic polymers were prepared, and different technologies were applied to select the suitable carrier and method. TBESD amorphous solid dispersion (TBESD-ASD) with polyvinylpyrrolidone K-30 was successfully prepared by the solvent evaporation method. The physicochemical properties of TBESD-ASD were investigated by scanning electron microscopy, differential scanning calorimetry, and Fourier-transform infrared spectroscopy. As a result, TBESD was found to be molecularly dispersed in the amorphous carrier. The solubilities and dissolution rates of all five ingredients in the TBESD-ASD were significantly increased (nearly 100% release), compared with raw TBESD. Meanwhile, TBESD-ASD showed good preservation stability for 3 months under accelerated conditions of 40 °C and 75% relative humidity. A subsequent pharmacokinetic study in rats revealed that  $C_{max}$  and  $AUC_{0-t}$  of all five components were significantly increased by the solid dispersion preparation. An *in vivo* study clearly revealed that compared to raw TBESD, a significant reduction in tumor size and microvascular density occurred after oral administration of TBESD-ASD to xenograft-bearing tumor mice. Collectively, the developed TBESD-ASD with the improved solubility, dissolution rates and oral bio-availabilities of the main ingredients could be a promising chemotherapeutic agent for cancer treatment.

### ARTICLE HISTORY

Received 12 November 2019  
Revised 6 January 2020  
Accepted 13 January 2020

### KEYWORDS

*Selaginella doederleinii*; biflavonoids; amorphous solid dispersions; polyvinylpyrrolidone K-30; oral bioavailability


## Introduction

*Selaginella doederleinii* Hieron, a medicinal herb that is widely distributed in Southern China and Southeast Asia, has been traditionally used as a folk medicine for the treatment of various cancers, especially for nasopharyngeal carcinoma, lung cancer, and cervical cancer (Liu et al., 2011; Sui et al., 2017; Yao et al., 2019). Nowadays, *S. doederleinii* was considered a complementary and alternative medicine in clinical practice due to its series of functional activities, referring to anti-oxidation (Saroni Arwa et al., 2015; Li et al., 2017), anti-inflammation (Kedi et al., 2018), anti-diabetic (Zheng et al., 2011), anti-virus (Coulerie et al., 2013), and anti-cancer effects (Li et al., 2014; Park & Kim, 2019). Phytochemical studies revealed that the chemical components of *S. doederleinii*

mainly consist of biflavonoids, such as amentoflavone, robustaflavone, 2'',3''-dihydro-3',3'''-biapigenin, 3',3'''-binaringenin, and delicaflavone (Li et al., 2013; Yu et al., 2017). Modern pharmacological studies have also revealed that the ethanol extract of *S. doederleinii* could induce cancer cells apoptosis, significantly inhibit the tumor growth, and enhance the anti-tumor immune response. However, this extract did not display oral acute toxicity *in vivo* (Sui et al., 2016). Due to including the abundant biflavonoids, the total biflavonoids extract of *S. doederleinii* (TBESD) had more powerful anti-cancer activities than its ethanol extract (Yao et al., 2017). Although, TBESD has shown many advantages, its low aqueous solubility, low gastrointestinal permeability, and poor oral absorption and bioavailability of the bioflavonoids in the

**CONTACT** Xinhua Lin  13906909638@163.com; Hong Yao  yauhong@126.com  Department of Pharmaceutical Analysis, Fujian Medical University, No. 1 Xueyuan Road, University Town, Fuzhou 350122, China; Jianyong Huang  Hjiy8191@163.com  Department of Pharmaceutics, Fujian Medical University Union Hospital, Fuzhou 350122, China

\*These authors contributed equally to this work.

 Supplemental data for this article can be accessed [here](#).

© 2020 The Author(s). Published by Informa UK Limited, trading as Taylor & Francis Group.

This is an Open Access article distributed under the terms of the Creative Commons Attribution-NonCommercial License (<http://creativecommons.org/licenses/by-nc/4.0/>), which permits unrestricted non-commercial use, distribution, and reproduction in any medium, provided the original work is properly cited.

extract posed problems in the drug delivery (Yang et al., 2016; Chen et al., 2018).

Drug delivery via the oral route is the most popular route owing to the safety, security, and simplicity of the administration. Investigations on the feasible oral drug delivery systems for water-insoluble drugs are still current hot spot issues (Mitrugotri et al., 2014; Papay et al., 2016). Several formulations, such as liposomes (Mignet et al., 2012), nanoparticles (Nam et al., 2018), self-nanoemulsifying drug delivery system (Tang et al., 2008; Yi & Zhang, 2019), and solid dispersions (Kanaujia et al., 2015; Wang et al., 2015), have been developed to enhance the aqueous solubility and oral bioavailability of these compounds. Among these preparation forms, solid dispersion is one of the most successful formulations for improving drug release and enhancing gastrointestinal absorption and oral bioavailability (Vo et al., 2013; He & Ho, 2015; Choi et al., 2016). Amorphous solid dispersions (ASDs) can be defined as molecular mixtures of hydrophobic drugs with a hydrophilic carrier that has a higher chemical potential energy than the corresponding crystalline forms, and can provide a solubility advantage over the crystalline form, without the involvement of any chemical changes to the compound (Li & Taylor, 2018; Wilson et al., 2018). Drug in solid dispersions could have a significantly higher solubility due to the amorphous state which could break the crystal lattice without the requirement of energy, and greater dissolution rate owing to an increase in surface area with a decrease in particle size (Vasconcelos et al., 2016; Iwashita et al., 2019). Therefore, Solid dispersions (SDs) are becoming a primary focus in the research and development, especially regarding the dosage forms used to establish water-insoluble active pharmaceutical ingredients (Zhang et al., 2018).

Amentoflavone, robustaflavone, 2'',3''-dihydro-3',3'''-biapigenin, 3',3'''-binaringenin, and delicaflavone are considered to be the primary herbal bioactive components that are responsible for the pharmacological action of TBESD (Yao et al., 2017). The major problems are the poor aqueous solubility and high lipophilicity for the TBESD ingredients with log *P* values ranging from 3.5 to 4.5, which ultimately limit the clinical utility owing to low bioavailability of the ingredients in the extract following oral administration (Chen et al., 2018). Therefore, it is important to develop a suitable formulation to ameliorate the solubility, dissolution rate, and bioavailability of TBESD. In recent years, a limited number of studies have reported the enhanced solubility and dissolution of the ingredients in TBESD. To the best of our knowledge, only few studies have been published on solid dispersions containing the *S. doederleinii* extract. Similar to general pharmaceuticals, the development of oral ASD formulations of TBESD, which primarily relies on optimizing suitable pharmaceutical carriers and technologies, is warranted. To overcome these issues, an optimal selection of excipients for TBESD amorphous solid dispersion (TBESD-ASD), which is the main factor involved in the physical stability and release behavior of the drug from the ASD, should be performed to determine the drug-excipient molecular interaction. The technologies used to produce SDs are classified as melting,

solvent evaporation, and melting-solvent methods (Paudel et al., 2013; Borba et al., 2016; Weerapol et al., 2017). As high temperatures during the melting process may induce the degradation or decomposition of the biflavonoids in TBESD, solvent evaporation was employed to prepare TBESD-ASD (Mohammadi et al., 2014).

In the current study, an ASD formulation was developed to ameliorate the solubility and dissolution rate of five major ingredients in the TBESD. Different excipients were tested to select the optimum carrier for TBESD-ASD using the solvent evaporation method. Finally, the ASD of TBESD was successfully formulated with polyvinylpyrrolidone K-30 (PVP K-30), one of the most common polymers used in commercial ASD formulations. The solid-state characteristics, dissolution behavior, and accelerated conditions for the stability of TBESD-ASD were investigated. Further, the oral bioavailability and antitumor effect *in vivo* were evaluated using an LC-ESI-MS/MS method and A549 xenograft-bearing mice models.

## Materials and methods

### Materials

TBESD was obtained from *S. doederleinii* using the reported methods (Yao et al., 2017); 103.82 mg/g, 37.52 mg/g, 44.40 mg/g, 53.36 mg/g, and 35.12 mg/g of amentoflavone, robustaflavone, 2'',3''-dihydro-3',3'''-biapigenin, 3',3'''-binaringenin, and delicaflavone were respectively used. Chrysin (purity  $\geq 98\%$ , internal standard, IS) was acquired from Shanghai Winherb Medical Technology Co., Ltd. (Shanghai, China). Reference standards for amentoflavone, robustaflavone, 2'',3''-dihydro-3',3'''-biapigenin, 3',3'''-binaringenin, and delicaflavone (purity  $\geq 98\%$ ) were isolated from *S. doederleinii* and their structures were fully elucidated by UV, MS,  $^1\text{H}$  NMR, and  $^{13}\text{C}$  NMR and confirmed by comparison to the literature (Li et al., 2014). The chemical structures of amentoflavone, robustaflavone, 2'',3''-dihydro-3',3'''-biapigenin, 3',3'''-binaringenin, and delicaflavone are shown in Figure S1.

Poloxamer 188, PVP K-30, and polyethylene glycol 4000 and 6000 (PEG 4000 and PEG 6000) were purchased from Sigma-Aldrich Co. (St. Louis MO). Acetonitrile (HPLC-grade) was supplied by Merck (Darmstadt, Germany). Acetic acid (HPLC-grade) was supplied by Aladdin (Shanghai, China). Ethanol (analytical grade) was purchased from Sinopharm Chemical Reagent Co., Ltd (Shanghai, China). All other chemicals were of analytical-grade or pharmaceutical-grade and were used without further purification.

### Sample preparation

*S. doederleinii* supplied by a local Chinese medical store in Fuzhou, China; the voucher specimens (no. 180708), and authenticated by professor Hong Yao (Department of Pharmaceutical Analysis, Fujian Medical University, Fuzhou, China), were stored in the Phytochemistry Laboratory.

TBESD was isolated from *S. doederleinii* using our previously described procedure (Yao et al., 2017). Briefly, after dried whole plants were pulverized into powder (20–40 mesh); the sample extracted at 85 °C for 2 h with an eightfold volume of 70% ethanol three times, and the resulting ethanol extracts were combined, transferred to a flask, and evaporated in a rotatory evaporator (Buchi, Flawil, Switzerland) to condense into a paste. The ethanol extract was extracted twice with petroleum ether and was then filtered. The residues were extracted twice with an eightfold volume of dichloromethane and were then filtered, and extracted twice with an eightfold volume of ethyl acetate and were filtered again. Ultimately, the ethyl acetate filtrate was concentrated using a rotary evaporator at 55 °C, and it was lyophilized to obtain TBESD.

Preparative fractionation of TBESD was performed on a 280 mL coil of 1.8 mm i.d. polytetrafluoroethylene and a 20 mL sample loop. The two-phase solvent system consisted of n-hexane-ethyl acetate-methanol-water 1:2:1.5:1.5. The coil column was first entirely filled with the upper phase; subsequently, the mobile lower phase was pumped (1 mL/min) into the head end of the inlet column. After reaching hydrodynamic equilibrium (850 rpm), the sample (500 mg) was dissolved in 20 mL of each two-phase solvent system and injected into the column through the injection valve.

### Content analysis of the main ingredients in TBESD

The amount of amentoflavone, robustaflavone, 2'',3''-dihydro-3',3'''-biapigenin, 3',3'''-binaringenin, and delicaflavone were determined with a Shimadzu LC-20AD HPLC system equipped with column Ultimate<sup>®</sup> XB-C18 (100 × 4.6 mm, 3.5 μm; Welch Materials, Inc., Ellicott, MD). The mobile phase consisted of water (containing 0.05% acetic acid, A) and acetonitrile (B) and was used at a flow rate of 1 mL/min. Column temperature was maintained at 30 °C, and detection wavelength was 270 nm. The quantification method from our previous report was applied (Chen et al., 2019). The following gradient elution program was used: 0–4 min, 30–40% B; 4–23 min, 40–42% B; 23–25 min, 42–46% B.

### Partition coefficients

The lipophilicity of the five major active ingredients in TBESD was evaluated by the shake-flask method, a standard procedure for testing the physicochemical property of chemicals (Organization for Economic Cooperation and Development (OECD), 2004; Ogden & Dorsey, 2019). The 1-octanol/water partition coefficients of the ingredients in TBESD were determined in a pH 7.4 buffer; in this method, double-distilled water and 1-octanol were used. Both solvents were mutually saturated at the temperature of the experiment prior to the performance of the experiments. Excess TBESD was added to 10.0 mL of aqueous buffer solutions and 10.0 mL of 1-octanol in glass flasks. The mixtures were shaken for 24 h at a constant temperature of 25 °C to achieve equilibrium. After centrifugation at 1000 × g for 5 min at 25 °C, the aqueous phases were isolated and the concentrations of amentoflavone,

robustaflavone, 2'',3''-dihydro-3',3'''-biapigenin, 3',3'''-binaringenin, and delicaflavone were determined by HPLC. The partition coefficients of five biflavonoids in TBESD were calculated using the following equation:

$$\log K_{ow} = \log C_o/C_w$$

where  $C_o$  is the concentration of biflavonoids in the 1-octanol phase at equilibrium;  $C_w$  is the concentration of biflavonoids in the aqueous phase at equilibrium;  $K_{ow}$  is the 1-octanol/water partition coefficients. All experiments were carried out at least in triplicate.

### Preparation of TBESD-ASD

A solid dispersion of TBESD with various polymers (Poloxamer 188, PVP K-30, PEG 4000, and PEG 6000) was prepared by the solvent method. The ratios of TBESD/polymers (w/w) are shown in Table 1. Briefly, the prescribed amounts of TBESD and polymer were separately dissolved in a certain volume of ethanol. The two solutions were mixed with ultrasonic stirring for 20 min, and then evaporated at 60 °C under vacuum to remove the solvent. The residue was evaporated to dryness under reduced pressure at 50 °C for 12 h. The dried samples were crushed and screened through a mesh size of 80. Prepared solid dispersions were kept in a desiccator until further investigation.

Several elements were considered during the preparation process for the TBESD-ASD. According to preliminary studies, the main variables that affect the solubility were ethanol concentration (%), mesh level (mesh), ultrasonic time (min), and drying temperature (°C) (labeled as A, B, C, and D in Table 2). In this study, an  $L_9$  ( $3^4$ ) orthogonal test design was employed to further optimize the preparation conditions for TBESD-ASD. The orthogonal design scheme was composed of four-factors and three-levels, totaling nine experimental groups, which is very effective and economical (Gao et al., 2012; Chen et al., 2019). The desirability function for the solubility of ASD was at the maximum level and was thus selected to optimize the TBESD-ASD formulation. In the current research, all data were determined as the mean of triplicate samples.

**Table 1.** Formulation of TBESD solid dispersions.

Ratio	TBESD (mg)	Polymer (mg)
1:3	20	60
1:4	20	80
1:5	20	100
1:10	20	200

**Table 2.** The factors and levels of orthogonal test.

	A	B	C	D
1	100	100	20	55
2	95	80	15	50
3	80	65	10	45

The amount of TBESD at 20 mg.

## Characterization of TBESD-ASD

### Morphology

Scanning electron microscopy (SEM) analysis of the TBESD and TBESD-ASD was performed using a Hitachi SU8010 microscope (Hitachi, Tokyo, Japan). The samples were attached to an aluminum sample holder using a double-sided adhesive tape.

### Differential scanning calorimetry

Differential scanning calorimetry (DSC) measurements were performed to examine the solid-state characteristics of TBESD, PVP K-30, PMs, and TBESD-ASD. Thermal analysis was carried out with STA 449 F3 Jupiter<sup>®</sup> (Netzsch, Selb, Germany). Samples were placed inside a crimped aluminum pan maintained at 25 °C for 5 min, and then heated to 300 °C at a heating rate of 10 °C/min.

### Powder X-ray diffraction (PXRD)

The crystalline state of TBESD, PVP K-30, PMs, and TBESD-ASD was evaluated using powder X-ray diffraction (DY5261/Xpert3, CEM, Matthews, NC). The samples were collected with a scan rate of 4°min<sup>-1</sup> in an angular range from 5° to 70° (2θ) using Cu Kα radiation (λ = 1.54 Å, wavelength) and operating at 40 kV and 40 mA.

### FT-IR spectroscopy

Infrared analysis of the solid complexes was carried out on a Nicolet IS5 (Thermo-Nicolet Instrument Co., Waltham, MA) at resolution of 4 cm<sup>-1</sup> over the range, 4000–500 cm<sup>-1</sup>. The FT-IR spectrograms of TBESD, PVP K-30, PMs, and TBESD-ASD were determined and compared.

### Solubility study

To evaluate the solubility of the ingredients in the ASD of TBESD with various polymers, an excess amount of ASD was added to 1 mL of distilled water. The effect of pH on the solubility of the ingredients in the ASD of TBESD with PVP K-30 was determined in 1 mL of PH 1.2, 4.5, and 6.8 buffers. In all cases, samples were placed in a thermostat oscillator and shaken for 48 h at 37 °C, and then centrifuged at 12,000×g for 15 min at 37 °C. After appropriate dilutions, the supernatants were subjected to HPLC. The experiments were carried out in triplicate.

### In vitro dissolution study

The dissolution studies were performed with a dissolution test apparatus III (ZRS-8GD, Tianjin, China) at a paddle speed of 100 rpm in 200 mL of 6.8 phosphate buffer maintained at 37 ± 0.5 °C (Chinese Pharmacopoeia Commission, 2015). Each formulation equivalent to 300 mg of TBESD was added to a dissolution vial. At predetermined time intervals (5, 10, 20, 30, 45, 60, 90, 120, and 180 min), 2 mL sample solution was withdrawn, and an equal volume of fresh medium was

replenished. The sample solution was centrifuged at 12,000×g for 5 min at 37 °C and the supernatants were subjected to HPLC.

### Stability study

The sample powder was stored in open transparent glass containers. The chemical stability test for the TBESD-ASD at 4500 ± 500 Lx illumination was carried out for 10 days to investigate the stability of the five components of TBESD in a strong light exposure environment.

The chemical stability test for the TBESD-ASD at 60 °C was carried out for 10 days to investigate the stability of the five components of TBESD in a high temperature environment.

The chemical stability test for the TBESD-ASD at 25 °C and 92.5% relative humidity (RH) was carried out for 10 days to investigate the stability of the five components of TBESD in a high humidity environment.

The chemical stability test for TBESD-ASD under accelerated (40 ± 2 °C/75 ± 5% RH) condition was carried out for 3 months to evaluate the preservation stability. The sample powder was enclosed into capsules in tightly capped brown glass vials to protect it from the light. At predetermined time intervals, sample powder was completely dissolved in ethanol and the five components content in TBESD-ASD were analyzed by HPLC.

### In vivo study

#### Animals

All animal experiments were approved by the Institutional Animal Care and Use Committee of Fujian Medical University. Animal welfare and experimental procedures were carried out following an approved protocol from the Guide for the Animals Care and the Ethics Committee of Fujian Medical University.

Eight-week-old Sprague-Dawley (SD) male rats ( $n = 12$ , 250 ± 20 g) were provided by the Laboratory Animal Center of Fujian Medical University. Six-week old BALB/c male nude mice ( $n = 36$ , 20 ± 2 g) were obtained from National Rodent Laboratory Animal Resource (Shanghai, China) and bred in the Laboratory Animal Center of Fujian Medical University. All rats were allowed to acclimatize to the laboratory conditions, including an ambient temperature of 25 ± 2 °C, a 12-h light/dark cycle, and an RH of 55 ± 5% over 1 week before the experiments. Rats were granted free access to food and water, and fasted with free access to water for 12 h before drug administration.

### Pharmacokinetic study

In this experiment, 12 male SD rats were randomly and equally divided into the TBESD group and a TBESD-ASD group ( $n = 6$ ). Thereafter, both groups were orally administered drugs that were equivalent to 20.76, 7.50, 8.88, 10.67, and 7.02 mg/kg for amentoflavone, robustaflavone, 2'',3''-dihydro-3',3'''-biapigenin, 3',3'''-binaringenin, and delicaflavone, respectively (200 mg/kg for TBESD). After



administration, 200  $\mu$ L of blood samples was obtained from the tail vein at 0, 3, 8, 15, 30, 45, 60, 90, 120, 240, 360, 480, 720, and 1440 min. All blood samples were immediately centrifuged at 3000 $\times$ *g* for 10 min at 4 °C. Thereafter, the supernatant was retrieved and stored at –80 °C until analysis.

Plasma samples were treated by the methanol deproteinization method and the plasma concentration of amentoflavone, robustaflavone, 2'',3''-dihydro-3',3'''-biapigenin, 3',3'''-binaringenin, and delicaflavone was analyzed using a previously developed LC-ESI-MS/MS method (Chen et al., 2018).

A highly sensitive and credible LC-ESI-MS/MS method was developed for the PK comparative study of TBESD and TBESD-ASD with simultaneous quantification of the five main biflavonoids in rat plasma. The pharmacokinetic parameters for free TBESD and TBESD-ASD were calculated by the non-compartmental method using the DAS pharmacokinetic software Version 3.0 (Bontz Inc., Beijing, China).

### Antitumor efficacy study

The xenograft-bearing mice model of A549 tumor was established by injecting of  $1.0 \times 10^7$  A549 cells via s.c. into the right front armpit area of BALB/c male athymic nude mice. Mice were randomly and equally divided into the vehicle control, TBESD, and TBESD-ASD groups when the xenograft tumors were palpable and had an average size of 80–100 mm<sup>3</sup> ( $n = 6$ ). The vehicle, TBESD (200 mg/kg), and TBESD-ASD groups (200 mg/kg) were administered p.o. every day for 16 days. The positive group was administered 2 mg/kg doxorubicin (Dox) i.v. once every three days via the tail-vein until sacrifice. Tumor size and body weight were measured and recorded every two days.

Tumor volume (*V*) was calculated using the formula:  $V = W^2 \times L / 2$ , where width (*W*) and length (*L*) were measured with an electronic caliper. Mice were killed one day following the last treatment, and tumors were collected, weighted, and photographed. The tumor inhibition effect was calculated using the following equation: tumor suppression (%) =  $(1 - T/C) \times 100$  where *T* represents the average tumor weight of the treated group and *C* represents that of the control group.

Immunohistochemistry (IHC) was carried out to further validate the antitumor efficacy of free TBESD and TBESD in the solid dispersion formulation *in vivo*. Tumors were collected and fixed in 4% neutral formalin for 24 h, and then embedded in paraffin. For the assessment of tumor microvessel density (MVD), some sections were deparaffinized and rehydrated. After quenching the endogenous peroxidase activity and blocking nonspecific binding sites, the slides were co-cultured with primary monoclonal CD34 antibody. For the quantification of positively stained vessels, the number of microvessels was counted in three randomly selected high-power fields by Image pro-plus software Version 6.0 at 200 $\times$  magnification.

### Statistical analysis

All data are expressed as mean  $\pm$  SD. Significance differences were derived by Student's *t*-test. \* $p < .05$  was considered to

indicate statistical significance while \*\* $p < .01$  was considered to indicate a highly significant difference.

## Results and discussion

### Partition coefficients

Before employing the formulation strategies to improve the solubility of poorly soluble drugs, the lipophilicity of the biflavonoids in TBESD should be considered. To address the first objective of this study, we measured the log *K*<sub>ow</sub> of five biflavonoids of TBESD in the normal internal environment pH buffers and compared our measurements to the predicted values of log *p* values obtained from Molinspiration Property Calculator (Molinspiration Cheminformatics, Bratislava, Slovak Republic) (Lipinski et al., 2001).

The lipophilicity is an important physicochemical property for characterizing the absorption, distribution, metabolism, and excretion (ADME) behavior of a drug. The results obtained for the five biflavonoids by the shake-flask method aligned well with the predicted values (Supplementary data, Table S1). However, their high Lipophilicity, with log *p* values ranging from 3.5 to 4.5, limit their absorption and bioavailability, as well as clinical utility. These findings suggest that a suitable formulation strategy must be developed to enhance the solubility and bioavailability of the main active ingredients in TBESD.

### Preparation of TBESD-ASD

Similar to general pharmaceuticals, the development of solid dispersions relies on having access to suitable pharmaceutical technologies and carriers to prepare the formulation (Yu et al., 2018). Previously, we demonstrated that the solvent evaporation method using anhydrous ethanol as a solvent enabled the successful development of TBESD-ASD. Depending on the properties of the carriers, different molecular weights and surface activity polymers have been reported to improve the solubility and concomitantly the dissolution rate of the hydrophobic drug in the solid dispersion (Weerapol et al., 2017). In this study, different polymers were evaluated to determine the optimal carrier for enhancing the solubility of all five components of TBESD when formulated as an ASD. All five components achieved the highest solubility among the screened polymers when the TBESD solid dispersion was formed with PVP K-30 (Figure 1). The enhanced solubility of amentoflavone, robustaflavone, 2'',3''-dihydro-3',3'''-biapigenin, 3',3'''-binaringenin, and delicaflavone owing to solid dispersion with PVP K-30 was 16.98-, 17.47-, 17.59-, 18.42-, and 19.48-fold higher than those of the biflavonoids for raw TBESD in water, respectively (Table 3). In addition, the nonhomogeneous and sticky mass solid dispersions were obtained by using Poloxamer 188, PEG 4000, and PEG 6000 as the carriers, might be due to the formation of a eutectic or monotectic mixture by the drug and polymer (Vippagunta et al., 2007; Brough and Williams, 2013). Altogether, it can be assumed that among the screened carriers, PVP K-30 exhibited better mobility, miscibility, and more similarity in the

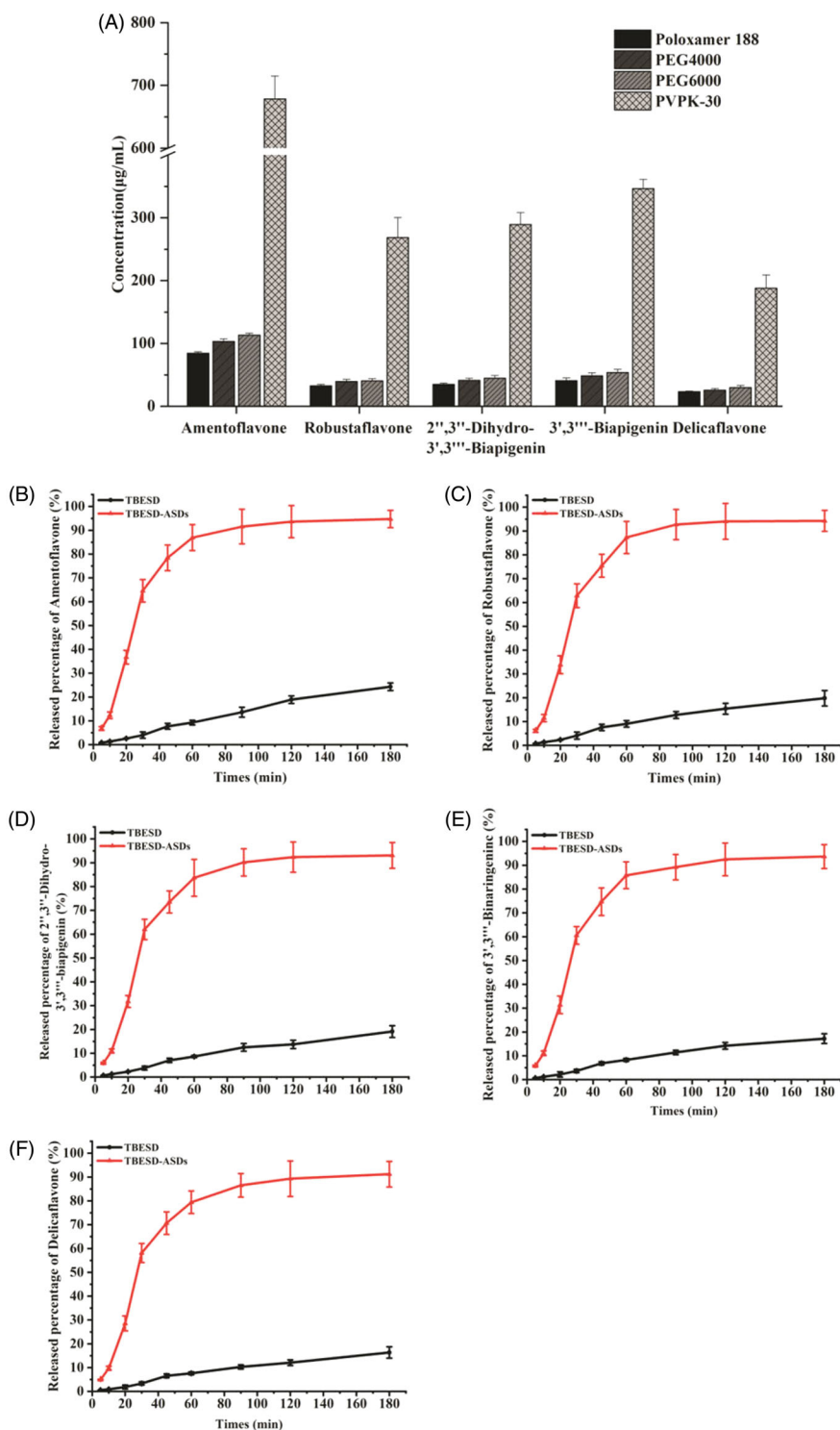


**Figure 1.** Solubility of the components of (A) TBESD after forming ASD with various polymers in distilled water at room temperature; Dissolution profiles of (B) amentoflavone, (C) robustaflavone, (D) 2'',3''-dihydro-3',3'''-biapigenin, (E) 3',3'''-binaringenin, and (F) delicaflavone from TBESD and solid dispersion formulations, respectively (mean  $\pm$  SD,  $n = 3$ ).

**Table 3.** Solubility from TBESD and ASDs with PVP K-30 in various pH medium at room temperature (mean  $\pm$  SD,  $n = 3$ ).

Solubility ( $\mu\text{g/mL}$ )	Components				
	Amentoflavone	Robustaflavone	2'',3''-Dihydro-3',3'''-biapigenin	3',3'''-Binaringenin	Delicaflavone
Pure extract in water	39.96 $\pm$ 2.46	15.37 $\pm$ 4.61	16.44 $\pm$ 3.47	18.71 $\pm$ 3.26	9.65 $\pm$ 1.03
ASDs in pH 1.2	434.15 $\pm$ 24.91	141.94 $\pm$ 17.15	178.65 $\pm$ 16.71	192.55 $\pm$ 21.46	112.54 $\pm$ 11.87
ASDs in pH 4.5	468.49 $\pm$ 27.16	168.39 $\pm$ 13.84	204.21 $\pm$ 19.46	243.67 $\pm$ 23.16	134.79 $\pm$ 10.13
ASDs in pH 6.8	615.69 $\pm$ 34.49	207.65 $\pm$ 21.89	246.32 $\pm$ 20.48	289.56 $\pm$ 28.13	175.16 $\pm$ 9.68
ASDs in water	678.38 $\pm$ 36.45	268.48 $\pm$ 31.73	289.16 $\pm$ 19.21	346.54 $\pm$ 14.56	187.98 $\pm$ 21.18

**Table 4.** Results of the orthogonal experiment ( $n = 3$ ).

	A	B	C	D	EE (%)
1	1	1	1	1	0.806
2	1	2	2	2	0.840
3	1	3	3	3	0.814
4	2	1	2	3	0.803
5	2	2	3	1	0.795
6	2	3	1	2	0.799
7	3	1	3	2	0.652
8	3	2	1	3	0.810
9	3	3	2	1	0.540
$K_1$	2.460	2.261	2.415	2.141	
$K_2$	2.397	2.445	2.183	2.291	
$K_3$	2.002	2.153	2.261	2.427	
$k_1 (=K_1/3)$	0.820	0.754	0.805	0.714	
$k_2 (=K_2/3)$	0.799	0.815	0.728	0.764	
$k_3 (=K_3/3)$	0.667	0.718	0.754	0.809	
$R$	0.153	0.097	0.077	0.095	
Optimal parameter	$A_1$	$B_2$	$C_1$	$D_3$	

$K_1$ ,  $K_2$ , and  $K_3$  are the sum scores of level 1, level 2, and level 3 for each factor.  $k_1$ ,  $k_2$ , and  $k_3$  are the average scores of level 1, level 2, and level 3 for each factor.  $R$  is the range among the average scores for each factor, estimated by the difference between the highest and the lowest score average ( $R = k_{\max} - k_{\min}$ ).

intermolecular interactions with the five biflavonoids. Hence, PVP K-30 was selected as the optimal polymers to form the TBESD-ASD for a further study.

Particle size reduction or generation of the amorphous states which could be significantly influenced on the surface area and solubility has attracted considerable attention (Onoue et al., 2011). Several factors influence the solubility of the ASD in the preparation process. In the current research, the preparation conditions of the ASD, including the ethanol concentration (%), mesh level (mesh), ultrasonic time (min), and drying temperature ( $^{\circ}\text{C}$ ), were optimized according to solubility by the orthogonal experiment design of  $L_9 (3^4)$ . To obtain high-quality TBESD-ASD with high solubility and appropriate particle size, the preparation conditions for the ASD were performed with four factors and three levels. The optimized compositions and the corresponding solubility of TBESD-ASD response values are listed in Table 4. The experimental results indicated that the ranking of the above factors was  $A > B > D > C$ . Consequently, the maximum value of the solubility was obtained when the ethanol concentration (%), mesh level (mesh), ultrasonic time (min), and drying temperature ( $^{\circ}\text{C}$ ) were 100%, 80 mesh, 20 min, and  $45^{\circ}\text{C}$  ( $A_1B_2C_1D_3$ ), respectively.

## Characterization of TBESD-ASD

### Morphology characteristics

The SEM micrographs of initial substances and TBESD-ASD exhibited clear morphological changes for the powder particles after ASD formation. Figure 2(A–C) shows the micrographs of TBESD, PVP K-30, and TBESD-ASD. The SEM image from the initial TBESD revealed an irregular shape with a rough surface. In contrast, the original PVP K-30 exhibited the typical spherical shape with a smooth surface. The TBESD-ASD also displayed the characteristic smooth surface. These results demonstrated that the formation of an ASD system containing TBESD resulted in a homogeneous dispersion of TBESD into the polymeric carrier.

## DSC results

DSC was employed in order to confirm the solid state of TBESD, PVP K-30, the physical mixtures (PMs) and TBESD-ASD. As shown in Figure 2(D), the DSC thermograms of TBESD displayed a broad endothermic peak at  $40\text{--}150^{\circ}\text{C}$ , with an endothermic peak at  $86.50^{\circ}\text{C}$ . PVP K-30 and PM (TBESD:PVP K-30 = 1:5) also exhibited an endothermic peak around  $63.50^{\circ}\text{C}$ . However, the DSC curves of TBESD-ASD displayed a shift in the endothermic peak to a slightly higher temperature of  $65.75^{\circ}\text{C}$ , as a TBESD peak was not observed, this indicates that TBESD was converted to an amorphous state and was thus dispersed in the molecular form in PVP K-30.

### Powder X-ray diffraction

X-ray diffractograms of TBESD, PVP K-30, PMs, and TBESD-ASD are shown in Figure 3(A). The PXRD pattern of TBESD showed a distinct peak at  $2\theta$  degree of 23.25, demonstrating the crystalline nature of TBESD. The characteristic crystalline peak observed in the diffraction PM patterns was missing in TBESD-ASD. These results suggest that there was a crystal transition of TBESD from the crystalline to the amorphous state in the SD.

### FT-IR spectroscopy

The infrared spectra of PVP K-30, the PMs, TBESD-ASD, and TBESD are shown in Figure 3(B). The presence of PVP K-30 was confirmed by the appearance of a peak at  $1662.37\text{ cm}^{-1}$  in the FTIR spectrum of the PMs, which corresponds to the  $\text{C}=\text{O}$  stretching of the pyrrolidone functional group unique to PVP K-30. However, the pyrrolidone peak in the TBESD-ASD was shifted slightly from  $1657.56\text{ cm}^{-1}$  observed in the ASD's spectrum due to the hydrogen bonded complex formation between PVP K-30 and biflavonoids in TBESD.

### Solubility study

The compounds in TBESD, including amentoflavone, robustaflavone,  $2'',3''$ -dihydro- $3',3'''$ -biapigenin,  $3',3'''$ -binaringenin, and delicaflavone, were analyzed by HPLC. As illustrated in Table 3, the solubility of the five major ingredients in pure TBESD was extremely low in water. However, all five ingredients in TBESD-ASD exhibited excellent solubility compared to free TBESD when formulated as an ASD with PVP K-30. The solid dispersion technique provided better wettability and dispersibility and successful enhancement of the solubility of the biflavonoids in TBESD. As is shown in Table 3, the compound solubility from TBESD-ASD displayed a profound increase with an increase in pH. Solubility of amentoflavone was 1.56-fold higher at neutral environments than the solubility found at pH 1.2. In contrast, robustaflavone,  $2'',3''$ -dihydro- $3',3'''$ -biapigenin,  $3',3'''$ -binaringenin, and delicaflavone respectively exhibited 1.89-, 1.62-, 1.80-, and 1.67-fold higher solubility. Such a significant increase in TBESD components' solubility, might be attributed to the changed glass transition temperature owing to the presence of hydrogen bonded network between PVP K-30 and TBESD (Roos et al., 2003).

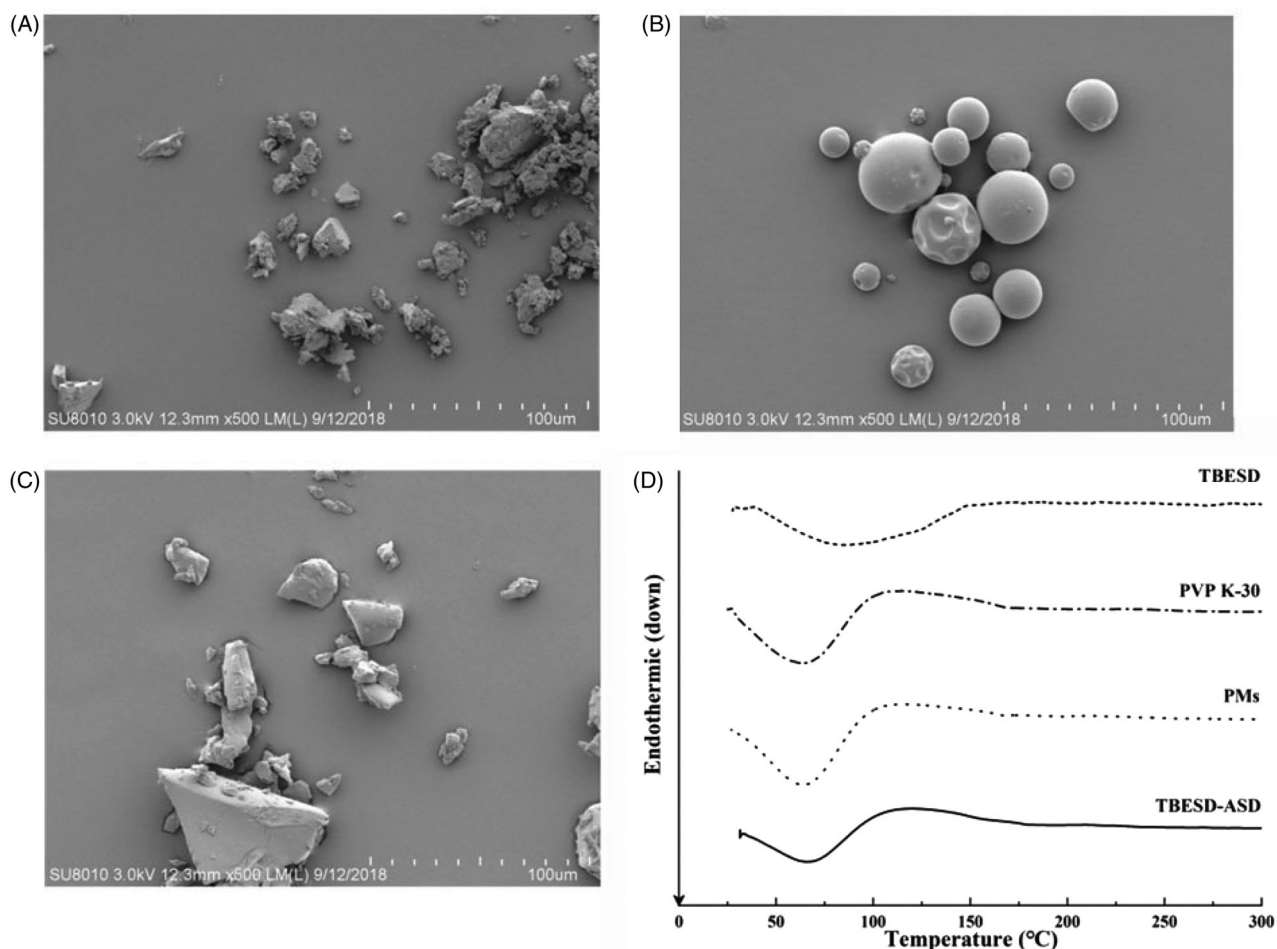


**Figure 2.** SEM images of (A) TBESD, (B) PVP K-30, and (C) TBESD-ASD; (D) DSC thermograms of TBESD, PVP K-30, PMs, and TBESD-ASD.

Therefore, TBESD-ASD can be enclosed into intestine-dissolved capsules which can be released and absorbed in a nearly neutral intestinal environment.

### In vitro dissolution study

The dissolution profiles of TBESD and TBESD-ASD were analyzed and the results are presented in Figure 1(B–F). Due to the low solubility of the five major biflavonoids in a pH 6.8 buffer, there was less than 25% release after 3 h. The cumulative amount of amentoflavone, robustaflavone, 2'',3''-dihydro-3',3'''-biapigenin, 3',3'''-binaringenin, and delicaflavone in the control group was 24.31%, 19.80%, 17.21%, 19.13%, and 16.35%, respectively.

The release rate of all five ingredients in TBESD-ASD was significantly higher than those in raw TBESD. After 60 min for the dissolution test, the release amount for amentoflavone, robustaflavone, 2'',3''-dihydro-3',3'''-biapigenin, 3',3'''-binaringenin, and delicaflavone released 86.91%, 87.29%, 83.66%, 85.79%, and 79.43%, respectively. At the end of the dissolution test, the release percentage for the five biflavonoids was 94.72%, 94.26%, 93.64%, 93.07%, and 91.22%, respectively. It was regarded as a full release and was significantly higher than that of TBESD. All results indicated that much faster and higher dissolution rates were obtained by TBESD-ASD compared with TBESD.

### Stability study

The presence of numerous ingredients in the herbal extract increases the risk of interactions among the components as well as degradation due to exterior conditions such as light, heat, and humidity. Therefore, the chemical stability of the herbal extract in the exterior environment should be investigated periodically.

In our preliminary experiment, the biflavonoids of the *S. doederleinii* extract displayed stability issues in the aqueous environment. The stability test for TBESD-ASD was carried out for 10 days and the results are shown in Figure 4. The content of the ingredients in TBESD-ASD was monitored in  $4500 \pm 500$  Lx illumination,  $60^\circ\text{C}$  and 92.5% RH conditions. Among the five ingredients in TBESD-ASD, 3',3'''-binaringenin and delicaflavone were especially unstable in a high temperature environment. In addition, the five biflavonoids of TBESD in ASD showed a relatively lower content than the ASD at 0 h in a strong light exposure environment. No significant difference was found for the loss of biflavonoids from the TBESD-ASD in the high humidity environment. This might be because the five major ingredients are flavonoids with potent anti-oxidative effects. The stability of TBESD-ASD enclosed in the capsules was investigated under accelerated ( $40 \pm 2^\circ\text{C}/75 \pm 5\%$  RH) conditions. As a result, no significant change in the content of all five biflavonoids in TBESD-ASD



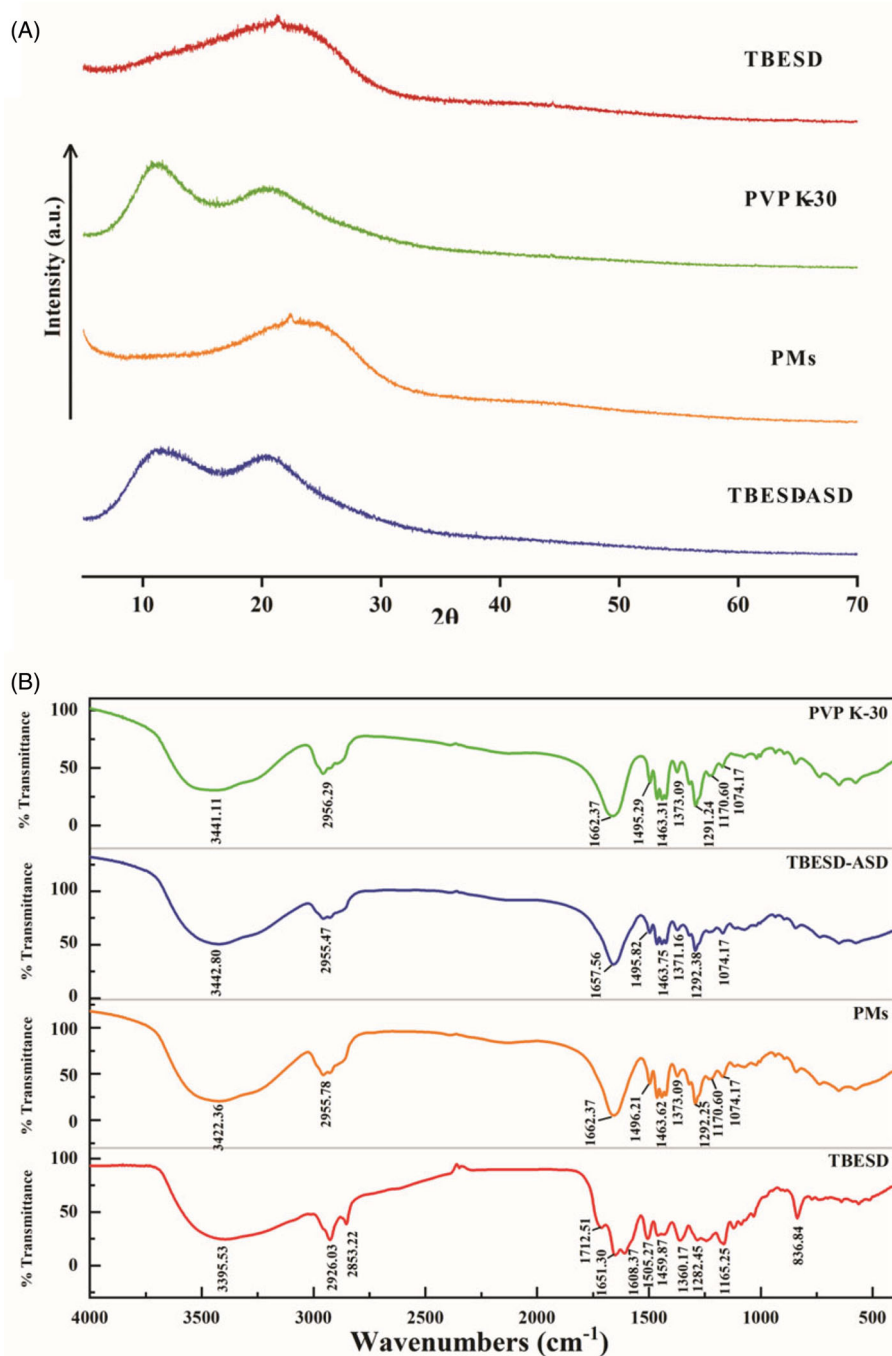


**Figure 3.** (A) PXRD patterns of TBESD, PVP K-30, PMs, and TBESD-ASD; (B) FT-IR spectra of TBESD, PVP K-30, PMs, and TBESD-ASD.

was found throughout the 90-day period (Supplementary data, Table S2). The solid dispersion technique can provide physical or steric hindrance, thereby preventing and reducing the rate of degradation of the active ingredients (Yu et al., 2017).

### In vivo study

#### Pharmacokinetic study

A comparative pharmacokinetic study was carried out in rats for the oral administration of raw TBESD and TBESD-ASD (200 mg/kg body weight as TBESD). Thereafter, the plasma

concentrations of the five biflavonoids were determined with a validated LC-ESI-MS/MS method. The plasma concentration–time curves for the studies ingredients in TBESD and TBESD-ASD are depicted in Figure 5, and the main PK parameters of the five biflavonoids are shown in Table 5. The plasma concentrations of the five active ingredients were significantly higher following oral administration of TBESD-ASD than TBESD. By comparing the PK parameters between TBESD-ASD and raw TBESD, we found that the mean  $C_{\max}$  and  $AUC_{0-t}$  of amentoflavone, robustaflavone, 2'',3'''-dihydro-3',3'''-biapigenin, 3',3'''-binaringenin, and delicaflavone in TBESD-ASD group were 3.43/2.78, 2.15/1.99, 3.97/3.72,

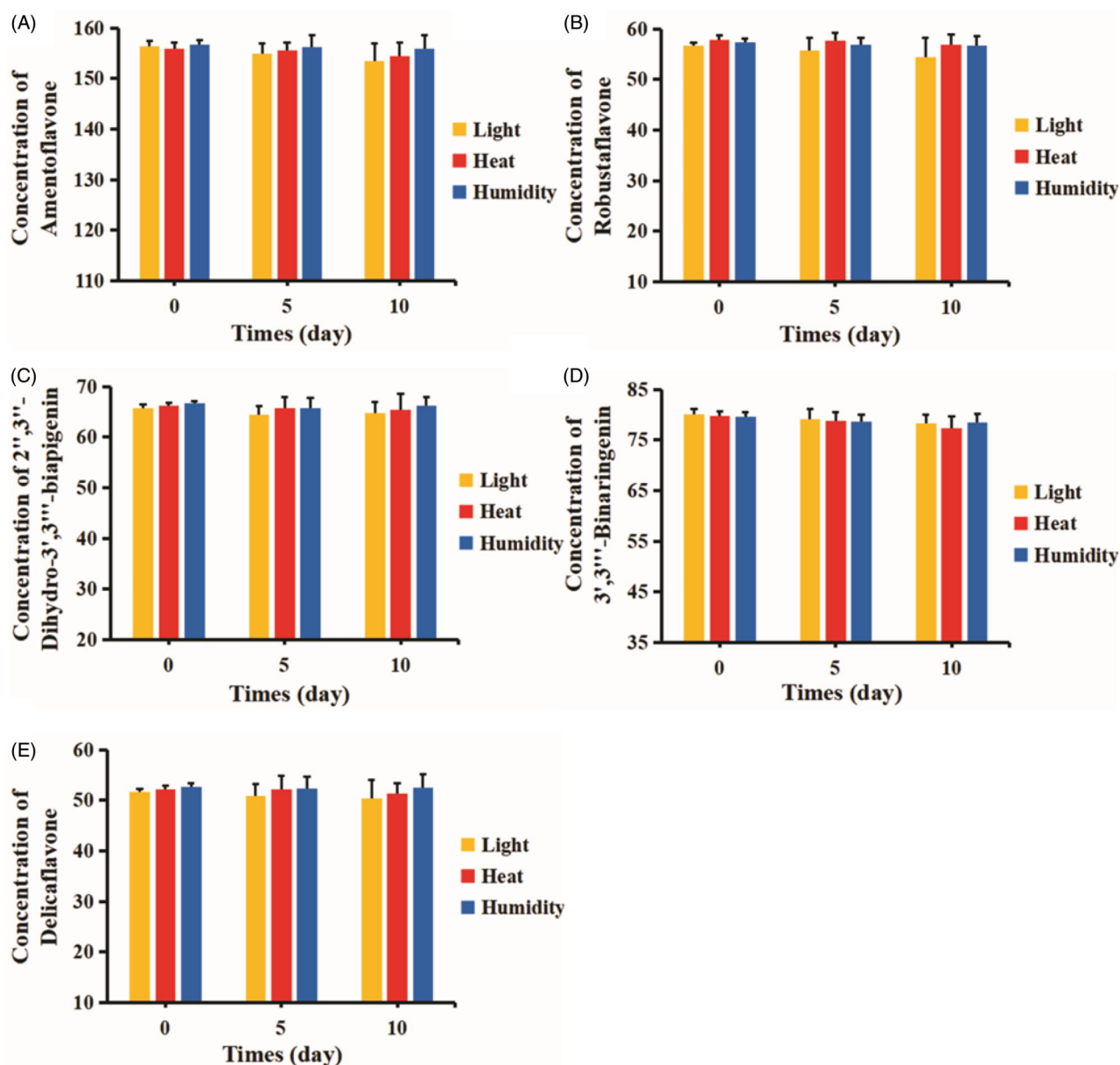


**Figure 4.** Chemical stability test of TBESD-ASD in difference exterior environment: (A) amentoflavone, (B) robustaflavone, (C) 2'',3''-dihydro-3',3'''-biapigenin, (D) 3',3'''-binaringenin, and (E) delicaflavone (mean  $\pm$  SD,  $n = 3$ ).

4.17/4.87, and 2.38/1.84-fold higher than those in the TBESD group, respectively. Such finding indicates that the absorption of the five active ingredients in the solid dispersion formulation substantially increased. Compared to the oral administration of TBESD, the  $MRT_{0-\infty}$  values of the five major active ingredients in the TBESD-ASD group were higher while their CL values were lower. The results indicated that the solid dispersion formulation increased blood retention times and decreased the elimination rates of the five biflavonoids from *S. doederleinii* (Yadav et al., 2019). Compared to the oral administration of TBESD, the relative bioavailability (RA) of amentoflavone, robustaflavone, 2'',3''-dihydro-3',3'''-biapigenin, 3',3'''-binaringenin, and delicaflavone from TBESD-ASD was 293%, 372%, 375%, 484%, and 278%, respectively. Thus, ASD was confirmed to be an effective oral formulation for TBESD formulation.

#### Antitumor efficacy study

The therapeutic efficacy of TBESD-ASD was evaluated in an A549 xenograft-bearing mice model, and treatment was initiated after tumors were fully established (when the tumor volume achieved an average size of 80–100 mm<sup>3</sup>).

Compared to the unrelenting growth in the control group, tumor volumes of mice in all treatment groups were significantly decreased ( $p < .01$ ). As shown in Figure 6(B), both the TBESD-ASD and Dox displayed superior antitumor effect relative to free TBESD and saline. As expected, treatment with Dox was effective at suppressing the tumor and this was accompanied by a significant loss in body weight. Mice were killed within 24 h after the last gavage, and their tumor tissues were collected and weighed (Figure 6(A)). The tumor growth inhibition (TGI) rates for the TBESD, TBESD-ASD, and Dox groups were 29.48%, 46.00%, and 58.44%, respectively

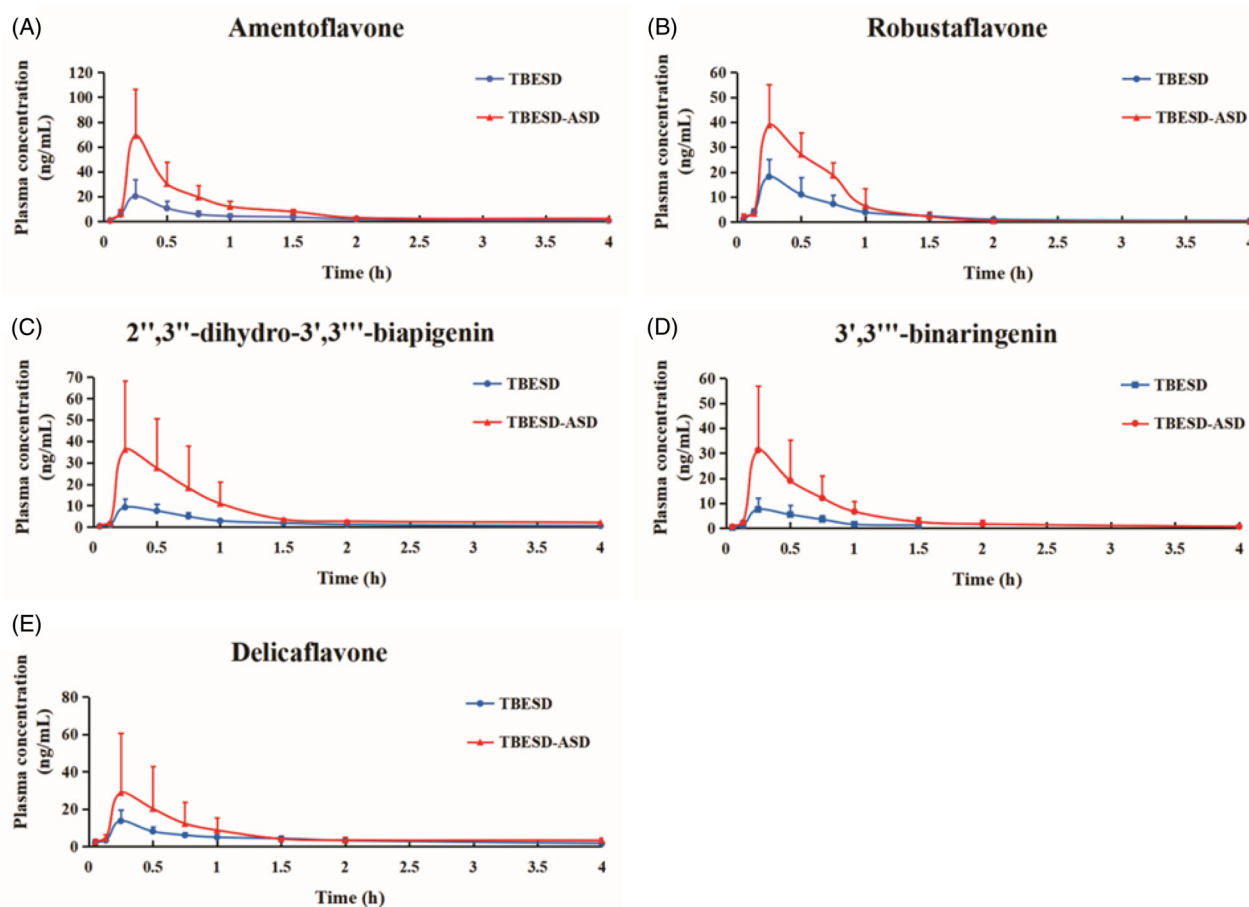


**Figure 5.** Mean concentration–time profiles of five active ingredients in rat plasma after a single oral administration of TBESD and solid dispersion formulations respectively (mean  $\pm$  SD,  $n = 6$ ).

**Table 5.** Pharmacokinetic parameters of five active ingredients in rats following single oral administration of TBESD and solid dispersion formulations, respectively (mean  $\pm$  SD,  $n = 6$ ).

PK parameters	Formulation	Amentoflavone	Robustaflavone	2'',3''-Dihydro-3',3'''-biapigenin	3',3'''-Binaringenin	Delicaflavone
$K_e$ ( $h^{-1}$ )	TBESD	1.31 $\pm$ 0.49	1.79 $\pm$ 0.40	1.23 $\pm$ 1.56	1.44 $\pm$ 0.59	0.37 $\pm$ 0.20
	TBESD-ASDs	1.15 $\pm$ 0.77	4.37 $\pm$ 5.72	0.55 $\pm$ 0.09 <sup>#</sup>	1.04 $\pm$ 0.69	0.38 $\pm$ 0.64
$t_{1/2}$ (h)	TBESD	1.00 $\pm$ 0.43	0.40 $\pm$ 0.09	1.18 $\pm$ 0.83	0.55 $\pm$ 0.20	1.06 $\pm$ 0.13
	TBESD-ASDs	1.09 $\pm$ 0.43	0.45 $\pm$ 0.41	1.30 $\pm$ 0.27*	0.74 $\pm$ 0.20	1.08 $\pm$ 0.37
$T_{max}$	TBESD	0.23 $\pm$ 0.05	0.25 $\pm$ 0.15	0.33 $\pm$ 0.13	0.27 $\pm$ 0.12	0.22 $\pm$ 0.06
	TBESD-ASDs	0.33 $\pm$ 0.13	0.22 $\pm$ 0.06	0.29 $\pm$ 0.10	0.23 $\pm$ 0.05	0.29 $\pm$ 0.10
$C_{max}$	TBESD	20.15 $\pm$ 13.35	18.09 $\pm$ 6.91	9.21 $\pm$ 3.93	7.48 $\pm$ 4.68	13.61 $\pm$ 5.81
	TBESD-ASDs	69.13 $\pm$ 37.63	38.87 $\pm$ 16.24*	36.16 $\pm$ 32.27 <sup>#</sup>	31.16 $\pm$ 25.82*	32.34 $\pm$ 33.36 <sup>#</sup>
$AUC_{0-t}$ (h· $\mu$ g/mL)	TBESD	14.83 $\pm$ 6.86	10.85 $\pm$ 5.41	9.52 $\pm$ 1.75	4.16 $\pm$ 2.28	18.08 $\pm$ 2.62
	TBESD-ASDs	41.30 $\pm$ 14.10*	21.59 $\pm$ 6.61*	35.43 $\pm$ 20.94*	20.26 $\pm$ 13.63*	33.26 $\pm$ 19.80 <sup>#</sup>
$AUC_{0-\infty}$ (h· $\mu$ g/mL)	TBESD	15.13 $\pm$ 6.68	11.66 $\pm$ 5.75	9.98 $\pm$ 1.62	5.75 $\pm$ 2.55	24.81 $\pm$ 9.30
	TBESD-ASDs	44.47 $\pm$ 13.14 <sup>#</sup>	28.75 $\pm$ 13.00*	39.43 $\pm$ 20.05*	24.53 $\pm$ 21.93*	65.35 $\pm$ 47.41 <sup>#</sup>
Cl (L/h)	TBESD	1530.83 $\pm$ 447.31	739.59 $\pm$ 257.35	909.15 $\pm$ 146.41	2170.42 $\pm$ 895.12	307.28 $\pm$ 78.42
	TBESD-ASDs	507.81 $\pm$ 171.52 <sup>#</sup>	323.06 $\pm$ 192.84*	289.20 $\pm$ 162.37 <sup>#</sup>	836.85 $\pm$ 696.73*	238.59 $\pm$ 320.60
$MRT_{0-\infty}$ (h)	TBESD	1.09 $\pm$ 0.29	0.61 $\pm$ 0.04	1.33 $\pm$ 0.72	0.52 $\pm$ 0.07	1.76 $\pm$ 0.44
	TBESD-ASDs	1.15 $\pm$ 0.53	0.53 $\pm$ 0.08	2.18 $\pm$ 0.80	0.89 $\pm$ 0.29 <sup>#</sup>	1.81 $\pm$ 0.95
RF		2.93	3.72	3.75	4.84	2.78

\*Indicates significant difference at  $p < 0.05$ . #Indicates significant difference at  $p < 0.01$ .

(Table 6). In particular, there was no significant difference in body weight between the TBESD-ASD treatment group and the TBESD treatment group. To further detect the antitumor effects of the TBESD solid dispersion formulation, the level of tumor angiogenesis blocking *in vivo* was analyzed via IHC of CD34. The control group displayed a high tumor MVD of  $96.24 \pm 6.91$  cells/mm<sup>2</sup>. As shown in Figure 6(D) and Table S3,

TBESD, TBESD-ASD, and Dox decreased the MVD counts of the xenografts tumor by 24.30%, 52.20%, and 59.91%, respectively. According to the MVD counts, the anti-tumor and anti-angiogenesis effects of TBESD-ASD were higher than those of free TBESD. Thus, we concluded that the TBESD-ASD is a promising formulation for exerting the therapeutic benefits of the bioactive ingredients in TBESD.

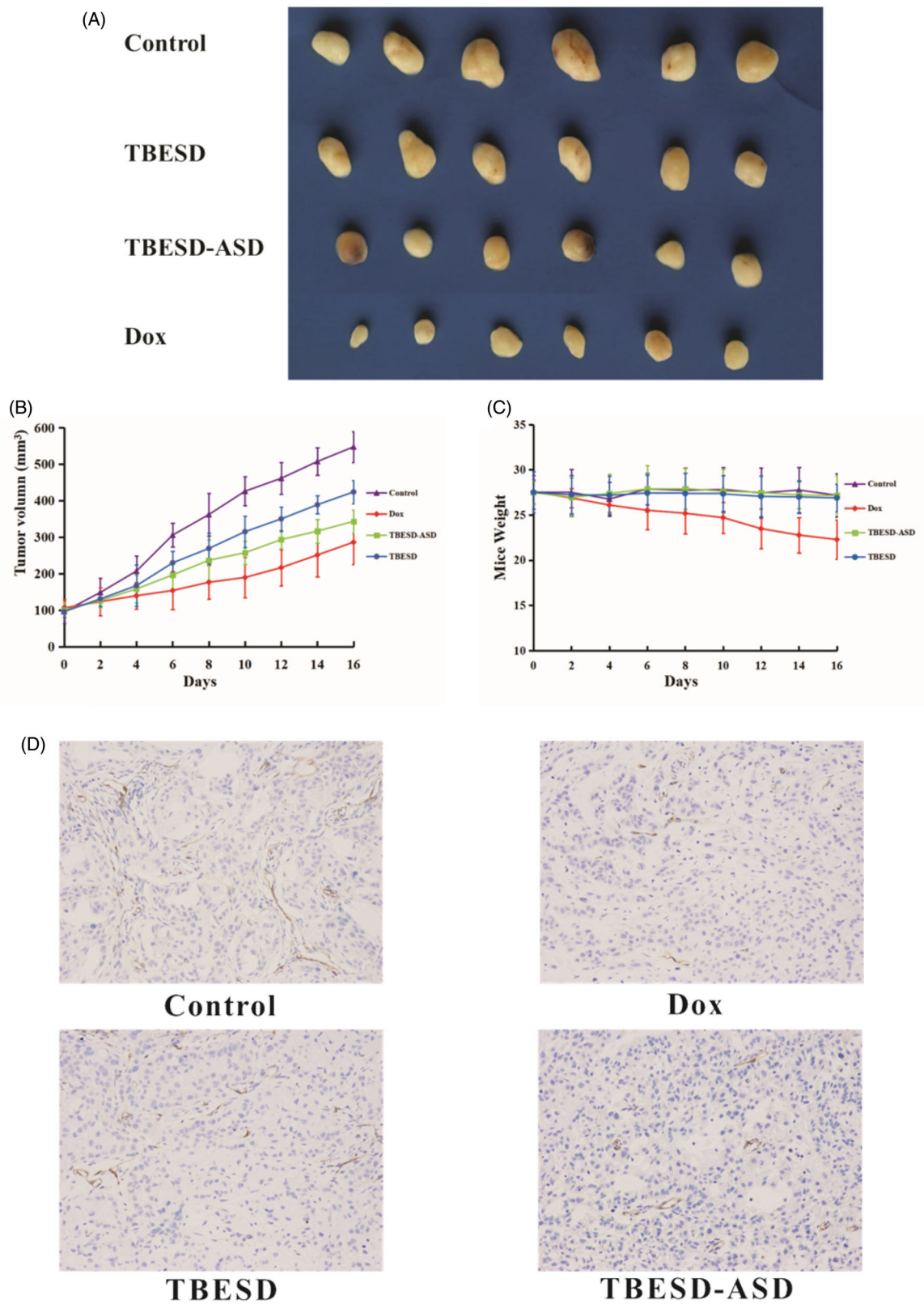


**Figure 6.** *In vivo* therapeutic study and Immunohistochemistry study of different TBESD formulations in a mice model. (A) Xenograft tumor in each group of mice after treatment, (B) xenograft tumor's growth curve of mice (mean  $\pm$  SD,  $n = 6$ ), (C) the average weight change of mice (mean  $\pm$  SD,  $n = 6$ ), and (D) representative CD34 staining ( $\times 200$ ) of xenograft tumor in each group.



**Table 6.** The average weights and tumor weight-inhibitions of mice before and after treatment (mean  $\pm$  SD,  $n=6$ ).

Groups	Dose (mg/kg)	Tumor weights (g)	Tumor weight-inhibitions (%)
Control	Solution	0.563 $\pm$ 0.187	–
Dox	2 mg/kg	0.244 $\pm$ 0.032**	58.44
TBESD	200 mg/kg	0.397 $\pm$ 0.049**	29.48
TBESD-ASDs	200 mg/kg	0.304 $\pm$ 0.042**	46.00

\*\*Indicates significant difference at  $p < 0.01$ .

## Conclusions

In the present study, an amorphous TBESD solid dispersion was successfully prepared by the solvent evaporation method and subsequently characterized. The solubility and dissolution rate of the five ingredients were significantly increased following the formation of the solid dispersion with PVP K-30, a suitable hydrophilic polymer and drug excipient. The composition of the formulation and the preparative technique were subsequently optimized using an  $L_9(3^4)$  orthogonal experimental design. The five major ingredients exhibited chemical stability over the 90 days of monitoring. During this period, the TBESD-ASD was stored as capsules under accelerated conditions. Pharmacokinetic evaluation of the amorphous nature of the TBESD solid dispersion showed that the oral bioavailability of amentoflavone, robustaflavone, 2'',3''-dihydro-3',3'''-biapigenin, 3',3'''-binaringenin, and delicaflavone were markedly improved and their RA reached 293%, 372%, 375%, 484%, and 278%, respectively. The significant increase in bioavailability was found to correspond with the increase in membrane permeability and bio-efficacy. In fact, the TBESD-ASD demonstrated greater antitumor effects than free TBESD, without systemic toxicity. These encouraging results suggest that ASD is an efficient drug delivery system for TBESD administration for cancer treatment, and could be a promising strategy for improving oral bioavailability and reducing the dose required for therapeutic efficacy.

## Acknowledgements

The authors thank the Fujian Medical University Ethics Committee for their kind guidance in the animal experiments.

## Disclosure statement

No potential conflict of interest was reported by the authors.

## Funding

The authors gratefully acknowledge the financial support of the National Natural Science Foundation of China (21775023 and 81973558), Joint Funds for the Innovation of Science and Technology of Fujian Province (2017Y9123, 2017Y9124, and 2018Y9076), Social Development Guiding Programs of Fujian Province of China (2017Y0042), Health and Youth Research Project of Fujian Province (2019-1-60), Funds for Scientific Research Startup of High-Level Talents of Fujian Medical University (XRCZX2018020), and Sailing Funds of Fujian Medical University (2018QH1016).

## References

- Borba PAA, Pinotti M, de Campos CEM, et al. (2016). Sodium alginate as a potential carrier in solid dispersion formulations to enhance dissolution rate and apparent water solubility of BCS II drugs. *Carbohydr Polym* 137:350–9.
- Brough C, Williams RO. (2013). Amorphous solid dispersions and nanocrystal technologies for poorly water-soluble drug delivery. *Int J Pharm* 453:157–66.
- Chen B, Wang X, Lin D, et al. (2019). Proliposomes for oral delivery of total biflavonoids extract from *Selaginella doederleinii*: formulation development, optimization, and in vitro–in vivo characterization. *Int J Nanomedicine* 14:6691–706.
- Chen B, Wang X, Zou Y, et al. (2018). Simultaneous quantification of five biflavonoids in rat plasma by LC-ESI-MS/MS and its application to a comparatively pharmacokinetic study of *Selaginella doederleinii* Hieron extract in rats. *J Pharm Biomed Anal* 149:80–8.
- Choi YH, Chin YW, Yang SJ, et al. (2016). Isolation of a lignan-enriched fraction from *Schisandra chinensis* and its effective solubilization via poloxamer 407-based solid dispersion formulation. *J Pharm Investig* 46:133–8.
- Chinese Pharmacopoeia Commission. 2015. Pharmacopoeia of the People's Republic of China. Shanghai, China: Chemical Technology Press.
- Coulerie P, Nour M, Maciuk A, et al. (2013). Structure-activity relationship study of biflavonoids on the Dengue virus polymerase DENV-NS5 RdRp. *Planta Med* 79:1313–8.
- Gao D, Tang S, Tong Q. (2012). Oleanolic acid liposomes with polyethylene glycol modification: promising antitumor drug delivery. *Int J Nanomed* 7:3517–26.
- He Y, Ho C. (2015). Amorphous solid dispersions: utilization and challenges in drug discovery and development. *J Pharm Sci* 104:3237–58.
- Iwashita M, Hashizume K, Umehara M, et al. (2019). Development of nobiletin-methyl hesperidin amorphous solid dispersion: novel application of methyl hesperidin as an excipient for hot-melt extrusion. *Int J Pharm* 558:215–24.
- Kanaujia P, Poovizhi P, Ng WK, Tan R. (2015). Amorphous formulations for dissolution and bioavailability enhancement of poorly soluble APIs. *Powder Technol* 285:2–15.
- Kedi PBE, Meva FE, Kotsedi L, et al. (2018). Eco-friendly synthesis, characterization, in vitro and in vivo anti-inflammatory activity of silver nanoparticle-mediated *Selaginella myosurus* aqueous extract. *Int J Nanomedicine* 13:8537–48.
- Li D, Qian Y, Tian YJ, et al. (2017). Optimization of ionic liquid-assisted extraction of biflavonoids from *Selaginella doederleinii* and evaluation of its antioxidant and antitumor activity. *Molecules* 22:586–602.
- Li N, Taylor LS. (2018). Tailoring supersaturation from amorphous solid dispersions. *J Control Release* 279:114–25.
- Li S, Yao H, Zhao M, et al. (2013). Determination of seven biflavones of *Selaginella doederleinii* by high performance liquid chromatography. *Anal Lett* 46:2835–45.
- Li S, Zhao M, Li Y, et al. (2014). Preparative isolation of six anti-tumour biflavonoids from *Selaginella doederleinii* Hieron by high-speed counter-current chromatography. *Phytochem Anal* 25:127–33.
- Lipinski CA, Lombardo F, Dominy BW, Feeney PJ. (2001). Experimental and computational approaches to estimate solubility and permeability in drug discovery and development settings. *Adv Drug Deliv Rev* 46:3–26.
- Liu H, Peng H, Ji Z, et al. (2011). Reactive oxygen species-mediated mitochondrial dysfunction is involved in apoptosis in human nasopharyngeal carcinoma CNE cells induced by *Selaginella doederleinii* extract. *J Ethnopharmacol* 138:184–91.
- Mignet N, Seguin J, Ramos Romano M, et al. (2012). Development of a liposomal formulation of the natural flavonoid fisetin. *Int J Pharm* 423:69–76.
- Mitragotri S, Burke PA, Langer R. (2014). Overcoming the challenges in administering biopharmaceuticals: formulation and delivery strategies. *Nat Rev Drug Discov* 13:655–72.
- Mohammadi G, Hemati V, Nikbakht MR, et al. (2014). In vitro and in vivo evaluation of clarithromycin–urea solid dispersions prepared by

- solvent evaporation, electrospraying and freeze drying methods. *Powder Technol* 257:168–74.
- Nam S, Lee SY, Kang WS, Cho HJ. (2018). Development of resveratrol-loaded herbal extract-based nanocomposites and their application to the therapy of ovarian cancer. *Nanomaterials* 8:384–97.
- Organization for Economic Cooperation and Development (OECD). 2004. Test no. 117: guideline for the testing of chemicals, partition coefficient (N-octanol/water): HPLC method.
- Ogden PB, Dorsey JG. (2019). Reversed phase HPLC with high temperature ethanol/water mobile phases as a green alternative method for the estimation of octanol/water partition coefficients. *J Chromatogr A* 1601:243–54.
- Onoue S, Uchida A, Takahashi H, et al. (2011). Development of high-energy amorphous solid dispersion of nanosized nobiletin, a citrus polymethoxylated flavone, with improved oral bioavailability. *J Pharm Sci* 100:3793–801.
- Papay ZE, Kallai-Szabo N, Ludanyi K, et al. (2016). Development of oral site-specific pellets containing flavonoid extract with antioxidant activity. *Eur J Pharm Sci* 95:161–9.
- Park HJ, Kim MM. (2019). Amentoflavone induces autophagy and modulates p53. *Cell J* 21:27–34.
- Paudel A, Worku ZA, Meeus J, et al. (2013). Manufacturing of solid dispersions of poorly water soluble drugs by spray drying: formulation and process considerations. *Int J Pharm* 453:253–84.
- Roos A, Chevallier C, Dormidontova EE, et al. (2003). Relation of glass transition temperature to the hydrogen bonding degree and energy in poly(N-vinyl pyrrolidone) blends with hydroxyl-containing plasticizers: 3. Analysis of two glass transition temperatures featured for PVP solutions in liquid poly(ethylene glycol). *Polymer* 44:1819–34.
- Saroni Arwa P, Zeraik ML, Ximenes VF, et al. (2015). Redox-active biflavonoids from *Garcinia brasiliensis* as inhibitors of neutrophil oxidative burst and human erythrocyte membrane damage. *J Ethnopharmacol* 174:410–8.
- Sui Y, Li S, Shi P, et al. (2016). Ethyl acetate extract from *Selaginella doederleinii* Hieron inhibits the growth of human lung cancer cells A549 via caspase-dependent apoptosis pathway. *J Ethnopharmacol* 190:261–71.
- Sui Y, Yao H, Li S, et al. (2017). Delicaflavone induces autophagic cell death in lung cancer via Akt/mTOR/p70S6K signaling pathway. *J Mol Med* 95:311–22.
- Tang J, Sun J, Cui F, et al. (2008). Self-emulsifying drug delivery systems for improving oral absorption of *Ginkgo biloba* extracts. *Drug Deliv* 15:477–84.
- Vasconcelos T, Marques S, das Neves J, Sarmiento B. (2016). Amorphous solid dispersions: rational selection of a manufacturing process. *Adv Drug Deliv Rev* 100:85–101.
- Vippagunta SR, Wang Z, Hornung S, Krill SL. (2007). Factors affecting the formation of eutectic solid dispersions and their dissolution behavior. *J Pharm Sci* 96:294–304.
- Vo CL, Park C, Lee BJ. (2013). Current trends and future perspectives of solid dispersions containing poorly water-soluble drugs. *Eur J Pharm Biopharm* 85:799–813.
- Wang W, Kang Q, Liu N, et al. (2015). Enhanced dissolution rate and oral bioavailability of *Ginkgo biloba* extract by preparing solid dispersion via hot-melt extrusion. *Fitoterapia* 102:189–97.
- Weerapol Y, Tubtimsri S, Jansakul C, Sriamornsak P. (2017). Improved dissolution of *Kaempferia parviflora* extract for oral administration by preparing solid dispersion via solvent evaporation. *Asian J Pharm Sci* 12:124–33.
- Wilson V, Lou X, Osterling DJ, et al. (2018). Relationship between amorphous solid dispersion in vivo absorption and in vitro dissolution: phase behavior during dissolution, speciation, and membrane mass transport. *J Control Release* 292:172–82.
- Yadav J, Korzekwa K, Nagar S. (2019). Impact of lipid partitioning on the design, analysis, and interpretation of microsomal time-dependent inactivation. *Drug Metab Dispos* 47:732–42.
- Yang S, Shi P, Huang X, et al. (2016). Pharmacokinetics, tissue distribution and protein binding studies of chrysoauloflavone I in rats. *Planta Med* 82:217–23.
- Yao H, Chen B, Zhang Y, et al. (2017). Analysis of the total biflavonoids extract from *Selaginella doederleinii* by HPLC-QTOF-MS and its in vitro and in vivo anticancer effects. *Molecules* 22:325–42.
- Yao W, Lin Z, Wang G, et al. (2019). Delicaflavone induces apoptosis via mitochondrial pathway accompanying G2/M cycle arrest and inhibition of MAPK signaling cascades in cervical cancer HeLa cells. *Phytomedicine* 62:152973–85.
- Yi T, Zhang J. (2019). Effects of hydrophilic carriers on structural transitions and in vitro properties of solid self-microemulsifying drug delivery systems. *Pharmaceutics* 11:267–80.
- Yu DG, Li JJ, Williams GR, Zhao M. (2018). Electrospun amorphous solid dispersions of poorly water-soluble drugs: a review. *J Control Release* 292:91–110.
- Yu H, Chang JS, Kim SY, et al. (2017). Enhancement of solubility and dissolution rate of baicalein, wogonin and oroxylin A extracted from *Radix scutellariae*. *Int J Pharm* 528:602–10.
- Yu S, Yan H, Zhang L, et al. (2017). A review on the phytochemistry, pharmacology, and pharmacokinetics of amentoflavone, a naturally-occurring biflavonoid. *Molecules* 22:299–322.
- Zhang Q, Polyakov NE, Chistyachenko YS, et al. (2018). Preparation of curcumin self-micelle solid dispersion with enhanced bioavailability and cytotoxic activity by mechanochemistry. *Drug Deliv* 25:198–209.
- Zheng XK, Zhang L, Wang WW, et al. (2011). Anti-diabetic activity and potential mechanism of total flavonoids of *Selaginella tamariscina* (Beauv.) Spring in rats induced by high fat diet and low dose STZ. *J Ethnopharmacol* 137:662–8.